ROYAL SOCIETY OF CHEMISTRY

www.rsc.org/crystengcomm

NOVEL COCRYSTALS OF GLICLAZIDE: CHARACTERIZATION AND EVALUATION

Renu Chadha*, Dimpy Rani, Parnika Goyal

University Institute of Pharmaceutical Sciences, Panjab University, Chandigarh-160014, INDIA

Email: ***renukchadha@rediffmail.com**

ABSTRACT

The present study involves exploration of the cocrystallization technique for amelioration of biopharmaceutical parameters of Gliclazide (GL), poorly water soluble anti-diabetic agent, using GRAS status coformers: succinic acid (GL-SA) and malic acid (GL-MA). Cocrystals were prepared by liquid assisted grinding and characterized by thermoanalytical and vibrational spectroscopic techniques. The crystal structure was determined from PXRD data using BIOVIA material studio software and further assessed for their solubility, intrinsic dissolution and *in-vivo* profile. Almost 2 fold improvement was observed in solubility and intrinsic dissolution. Pharmacodynamic and pharmacokinetic studies evidenced remarkable reduction in glucose level and higher C_{max} in comparison to GL, respectively. The new solid entities, thus formed, have the potential to be developed as a new formulation of GL and can be commercialized.

INTRODUCTION

One of the challenges faced during the drug development process by a drug molecule is its bioavailability, which in turn is dependent on the solubility of the drug molecule [1,2]. This parameter can be successfully controlled by a collection of non-covalent interactions creating the roots for diversity in pharmaceutical solid-state forms of the same molecules [3]. So awareness and research into solid-state characteristics and physicochemical properties of drug molecule is a fundamental step in designing a drug and its performance [4].

One of the prolific methods involving non-covalent interactions, to improve physicochemical properties is cocrystallization. Pharmaceutical cocrystals are one of the subcategories of a broader group of multicomponent crystals that also includes inclusion complexes, salts, solvates and hydrates [5]. They consist of at least two components (API and coformer) interacting in a crystal lattice via non-covalent bonding primarily hydrogen bonding and hold distinctive crystalline structure with unique properties while retaining the intrinsic activity of the parent API [6,7]. This technology is widely being used to develop new crystal forms of many active pharmaceutical ingredients [5-9].

The present work describes the cocrystallization of gliclazide (GL) (pKa 5.8)[10] (Figure 1a), a second generation sulfonyl urea, widely used in non-insulin dependent diabetes. Unfortunately, this drug is practically insoluble which further affects its bioavailablity. Many groups of workers have attempted to improve solubility using various approaches such as preparing cyclodextrin complexes [11-14], solid dispersions [15-18] and nanoparticles [19-21]. However, no report has appeared about the cocrystal of this therapeutically useful molecule.

(a)   (b)   (c)
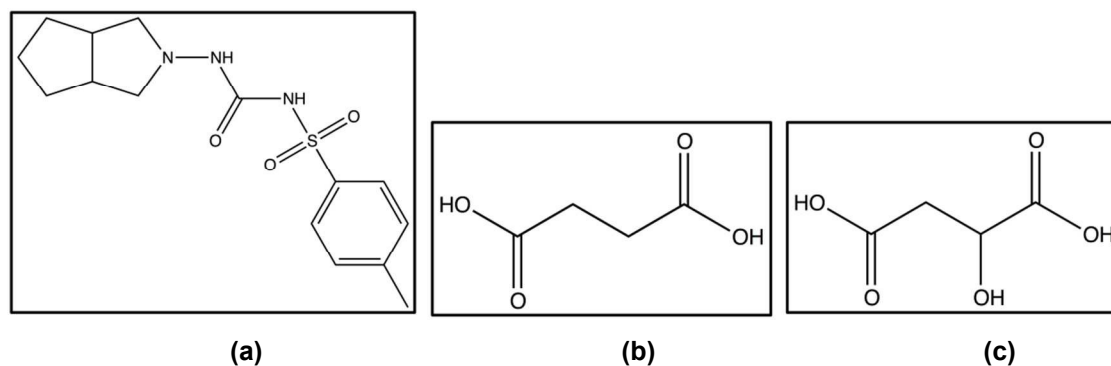
Figure 1 (a) Chemical structure of GL, (b) SA, (c) MA

GRAS status coformers, Succinic acid (SA) (Figure 1b) and Malic acid (MA), (Figure 1c) has been used. The cocrystals, thus formed, were characterized using various analytical techniques and were subjected to *in-vitro* and *in-vivo* studies to evaluate their efficacy.

EXPERIMENTAL

Materials

GL (≥99%, Ind Swift Ltd, Panchkula, India), SA (≥98%, Central Drug House Ltd, New Delhi, India), MA (≥98%, Central Drug House Ltd, New Delhi, India), Ethanol (≥99.8%, E. Merck Ltd, Mumbai, India) and acetone (≥99.8%, E. Merck Ltd, Mumbai, India) were purchased and used as received.

Sample Preparation

Two cocrystals, GL-SA and GL-MA were prepared by liquid assisted grinding. A 1:1 mixture of GL (32.341 mg) with SA (11.809 mg) and MA (13.408 mg) was ground in pestle mortar by adding ethanol (5 ml) and acetone (10 ml) respectively, drop by drop up to 60 minutes at room temperature. The recrystallization through solution method was also attempted, but crystals with suitable size and good diffraction quality were not isolated for single crystal X-ray diffraction analysis.

Differential Scanning Calorimetry (DSC)

DSC was recorded on Q 20 (TA-Instruments Inc., USA) at a heating rate of 10 °C/min in the temperature range 25-250°C, under a dry nitrogen atmosphere (flow rate of 50 ml/min). DSC was calibrated with indium (99.99% purity, mp 156.6 °C) and aluminium pans were used for samples and references. The data was integrated with Universal Analysis 2000 software (TA Instruments Inc.).

Fourier Transform Infrared Spectroscopy (FTIR)

FTIR spectras were collected using spectrum two IR spectrometer (Perkin Elmer, England). The samples were prepared by KBr pellet technique and analyzed over the wavenumber range of 400–4000 cm−1 with 4 accumulative scans having resolution of 4 cm−1.

Powder X-ray Diffraction (PXRD)

PXRD diffraction patterns were collected from using X-ray diffractometer PANalytical X'Pert Pro X-ray powder diffractometer (The Netherlands, Holland). The operating conditions were as follows: Cu Kα radiation at 40 kV and 45 mA, analyzed from 5°-45° (2θ), angular range 5, fixed divergence slit, scan rate 0.00085°/sec, high resolution. The data were analyzed by X'PERT high Score software.

Crystal Structure Determination from PXRD

The crystal structure was determined from its PXRD pattern using Reflux Plus module of Material studio (BIOVIA 7.0), as crystals of good quality were not collected. The position of peaks (5°-40° 2θ) in the powder diffraction pattern were indexed using X-cell to depict the crystal unit cell and approximate lattice parameters. Pawley refinement of the peak profiles was then performed until the figure of merit reached a good quality of fit. Geometrically optimized structure (using DMol3) of drug and coformer were introduced into the empty unit cell so obtained and subjected to Powder solve using a simulated annealing algorithm, followed by Rietveld refinement and was geometrically optimized.

Enthalpy of Solution

Enthalpy of solution of the samples was determined by Isoperibol Solution Calorimetry (Calorimetry Science Corporation, UTAH, USA) model 4300 in phosphate buffer at pH 7.4 at 37°C with stirring at 100 revolutions/min [23].

Equilibrium Solubility Studies

The equilibrium solubility study was performed by shaking an excess amount of drug (approx 20 mg) in 10 ml phosphate buffer of pH 7.4 (recommended media in USP XXV), in water bath shaker MSW-275 Macroscientific works, Delhi at 37°C for 24 hours at 200 rpm. The resulting slurry was filtered through 0.45μm membrane filter and absorbance was measured at 224.8 nm with Lambda 25 UV/VIS spectrometer to determine the concentration.

Intrinsic Dissolution Studies

Intrinsic dissolution study was performed with rotating disk dissolution test apparatus, DS 8000 (Lab India Analyticals) in phosphate buffer pH 7.4 (recommended media in USP XXV) at 37°C with 100 rpm for 4 hours. A pellet of the sample was formed with the help of die and punch, compressed by tablet press and attached to dissolution apparatus holder and immersed in dissolution media. 10 ml of phosphate buffer pH 7.4 with replacement was withdrawn at different intervals of time and filtered through 0.45μm membrane filter. The concentration was determined by measuring absorbance at 224.8 nm with Lambda 25 UV/VIS spectrometer. Intrinsic dissolution rate was expressed in ± SD values.

***In Vivo* Studies**

4-5 week old male Wistar rats (150-250 g) were procured, kept in the Central Animal House and provided with standard pellet diet and water *ad libtum*. Diabetes was induced by a single dose of streptozotocin plus nicotinamide solution (45 mg/kg) prepared in citrate buffer (pH 4.4, 0.1 M) intraperitoneally [24-25]. The animals were diabetic within 48 hours after injection. The rats were divided into 5 groups and each group consist of 6 rats (n=6).

For pharmacodynamic study, GL, GL-SA and GL-MA (dose 40 mg/kg) were suspended in citrate buffer (pH 4.4, 0.1 M) and administered orally for 7 days. The plasma glucose level was checked in protein free plasma by enzymatic GOD – POD (glucose oxidase peroxidase) method after 7 days. Concentration of glucose was represented by mean ± SEM and pharmacodynamic data of cocrystals were compared with drug, non diabetic control and diabetic control group by One-way ANOVA followed by Dunnett's test and Student's t test using GraphPad Prism 6.0 software at 95% confidence interval.

Pharmacokinetic study[26] was performed on normal rats and sampling was done up to 24 hours at different intervals. GL, GL-SA and GL-MA (dose 40 mg/kg) were suspended in normal saline and a single dose was administered orally to each group. Plasma concentration at different intervals were analyzed by HPLC. Peak plasma concentration (C_{max}) was calculated by PKSolver: An Add–in program [27], which does the calculation based on the linear trapezoidal method. Concentration of GL was represented by mean ± SEM and pharmacokinetic data of cocrystals were compared with GL and control group by One-way ANOVA followed by Dunnett's test and Student's t-test using GraphPad Prism 6.0 software at 95% confidence interval.

HPLC Studies

The concentration of GL was determined by Waters Alliance HPLC system which includes a waters 2996 Photodiode Array Detector and a 4.6 mm × 150 mm SunFire[TM] C_{18}, 5 µm column (Waters Corporation, Milford, MA). Calibration curve was plotted by spiking different concentrations of GL in plasma. All the samples of 10 µl injection size were run by isocratic mobile phase which consisted of acetonitrile: water (50:50) of pH 3 (pH was adjusted with orthophosphoric acid) with flow rate 1.2 ml/min. GL peak was detected at 228 nm with retention time 5.8 min.

RESULTS AND DISCUSSION

DSC Thermal Analysis

Single, sharp and narrow endothermic peaks of GL-SA and GL-MA appeared at 135.17ºC and 157.26ºC, respectively (Figure 2) in the DSC thermogram, which is considerably different from melting endotherms of GL (171.04 ºC) and corresponding coformers (SA at 192.29 and MA at 135.23 ºC), implying generation of a new crystal phase. The melting of GL-MA, positioned amid the melting endotherms of GL and MA, indicating the likelihood of cocrystal whereas melting endotherm of GL-SA appeared before the melting of GL and SA, suggesting the formation of either cocrystal or eutectic. However, DSC of physical mixture (supplementary data, Figure S1) presented two broad peaks different from that of GL-SA. This negates the existence of eutectic and confirms possibility of cocrystal.
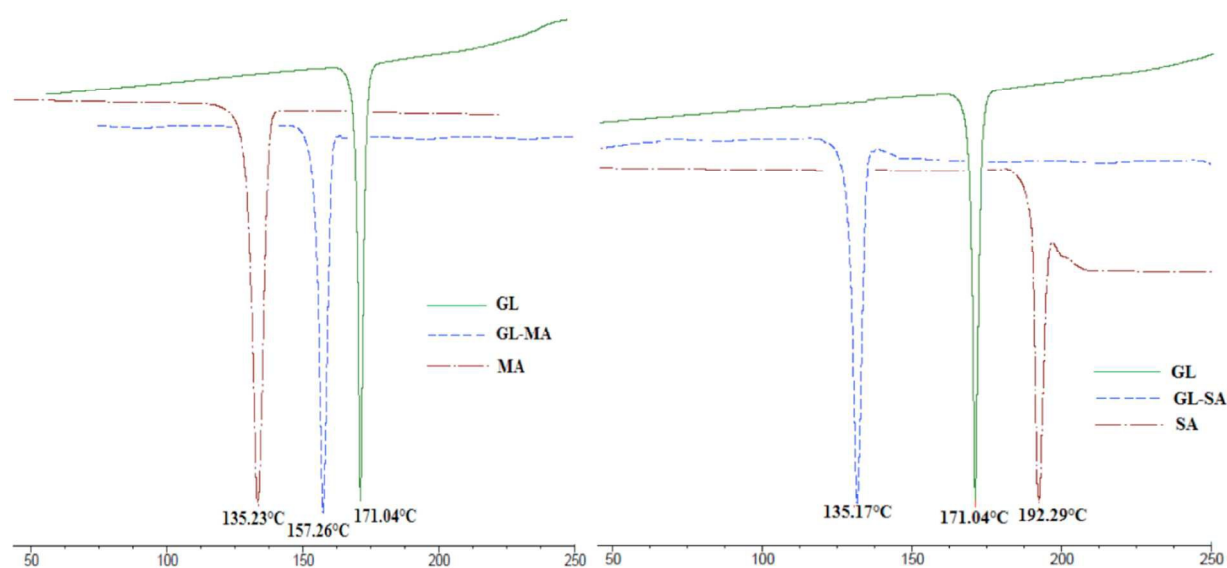
Figure 2 DSC of GL, coformers, GL-SA and GL-MA

FTIR spectroscopy

FTIR is an excellent analytical technique to study the changes in the vibrational modes of the functional groups that participate in cocrystal formation. In IR spectrum of GL-SA, significant shifts were seen in both the sulfamoyl and hydroxyl region of GL and SA, respectively. A major shift was observed in the -SO_2 stretch of GL, from 1163 and 1349 cm^{-1} to 1157 and 1342 cm^{-1}, respectively, while –OH of carboxylic group of SA shifted from 3209 cm^{-1} to 3198 cm^{-1}, inferring interaction between these two regions in GL-SA (Figure 3). In case of GL-MA, the peaks of GL shifted from 3273 cm^{-1} to 3269 cm^{-1} (-NH stretch of sulfamoyl), 1349 and 1163 cm^{-1} to 1345 and 1158 cm^{-1} (-SO_2 stretch of sulfamoyl), respectively and 1709 cm^{-1} to 1702 cm^{-1} (–CO stretch of carbamoyl), accompanied by shift in –OH and –CO of carboxylic group of MA from 3448 and 1691 cm^{-1} to 3443 and 1686 cm^{-1}, respectively. It is evident from the shift of peaks

to the lower side, that these groups are involved in forming the intermolecular hydrogen bonds between

GL and the coformers, resulting in formation of cocrystals.
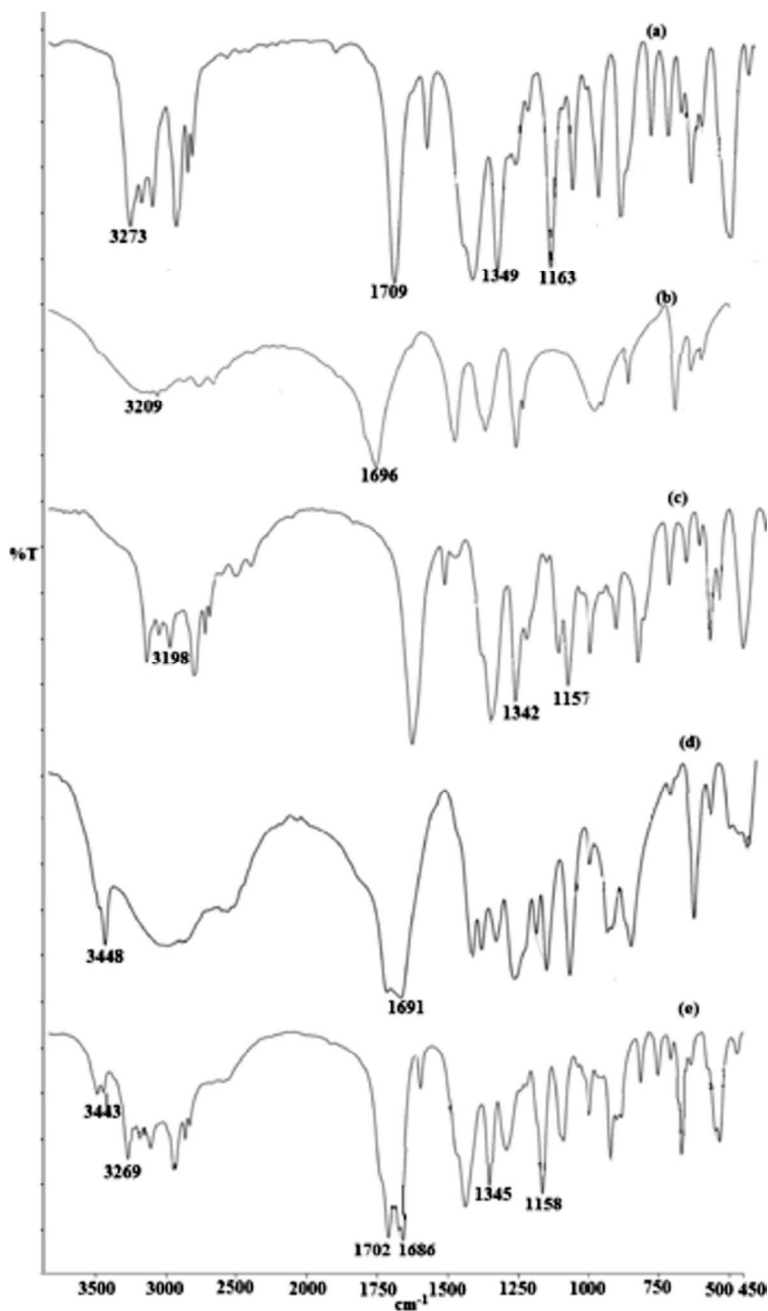
Figure 3 FTIR spectra of (i) (a) GL (b) SA (c) GL-SA (d) MA (e) GL-MA

PXRD Analysis

PXRD is a reliable tool to gain qualitative information pertaining to the interaction of the solids. The peaks

generated in the PXRD are the fingerprint for the crystalline phase. Any event of disappearance of peaks,

appearance of new peaks or distortion in peaks, gives an estimate that two solid systems are interacting together and forming a new solid system that is different from parent solid constituents.

The formation of a new solid phase in GL-SA and GL-MA is confirmed by the noticeable differences in the diffraction pattern, in comparison to GL, which are observed mainly in the 2θ region of 12° - 40°.

In GL-SA (Figure 4), certain characteristic peaks of GL at 18.40° and 21.90° have disappeared while some peaks from 25.34°, 42.45°, and 43.39° have shifted significantly to 25.46°, 42.05° and 43.52° respectively. The characteristic peak (100% relative intensity) of SA at 20.12° has merged with a peak of GL at 20.20° to give a single peak at 20.01°. Along with it, another peak present in both GL and SA at 26.26°, shifted to a new position *i.e.*, at 26.14°. A peak at 40.74°, present in SA, has also been disappeared in the cocrystal. Apart from this, the PXRD of GL-SA has also witnessed the appearance of peaks at 31.52°, 38.01°, which are new to both GL and SA.

Similarly, In the GL-MA (Figure 4), significant changes have been observed in the PXRD pattern. In cocrystal, certain distinctive peaks of GL at 20.43° and 21.90° have disappeared while some peaks from 30.09°, 38.56° and 43.39° have shifted considerably to 30.26°, 38.65° and 43.51°, respectively. Beside this, three peaks present in GL at 20.20°, 23.77° and 37.10° amalgamated with three peaks in MA positioned at 20.20, 23.65° and 37.60 respectively, merge to give exclusive peaks at 20.23°, 23.60° and 37.48° correspondingly. Beside this, there is a small shift in the position of two peaks of MA, from 27.72° and 32.90° to 27.64 and 32.79°, respectively. Moreover, a new peak at 22.74° also has been observed.

Thus, all these noticeable changes in the obtained PXRD patterns of Gl-SA and GL-MA, in comparison to drug and coformers, infer the formation of cocrystals.
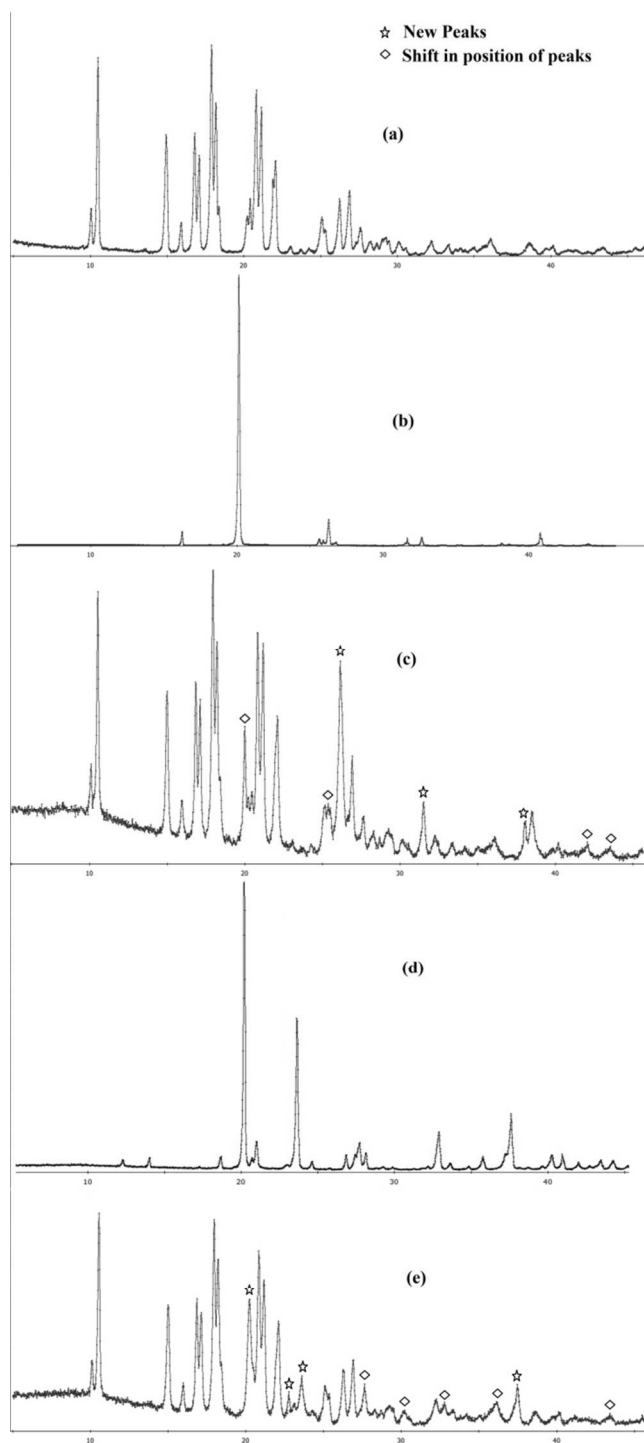
Figure 4 PXRD pattern of (a) GL (b) SA (c) GL-SA (d) MA (e) GL-MA

Crystal structure determination from PXRD

The crystal structure of GL-SA and GL-MA was determined using PXRD, as described in experimental section.

These cocrystals are formed as a result of heteromeric interactions between GL and coformers by replacing homomeric interaction in GL [22] as shown in figure 5.
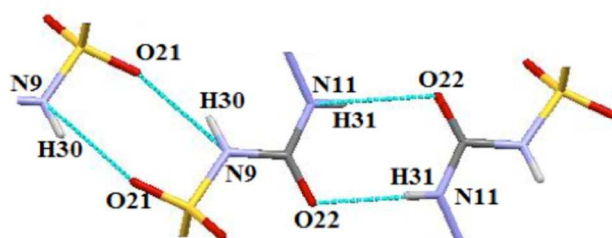
Figure 5 Homomeric interactions in GL [22]

GL-SA crystallizes in the triclinic system with the space group P_1 (R_{wp} = 14.71, Figure 6). The asymmetric unit and packing pattern is given in figure 7. SA is attached to GL through hydrogen bond, O51–H56···O20 while all asymmetric units are held together by Vander Waals forces (Figure 7).
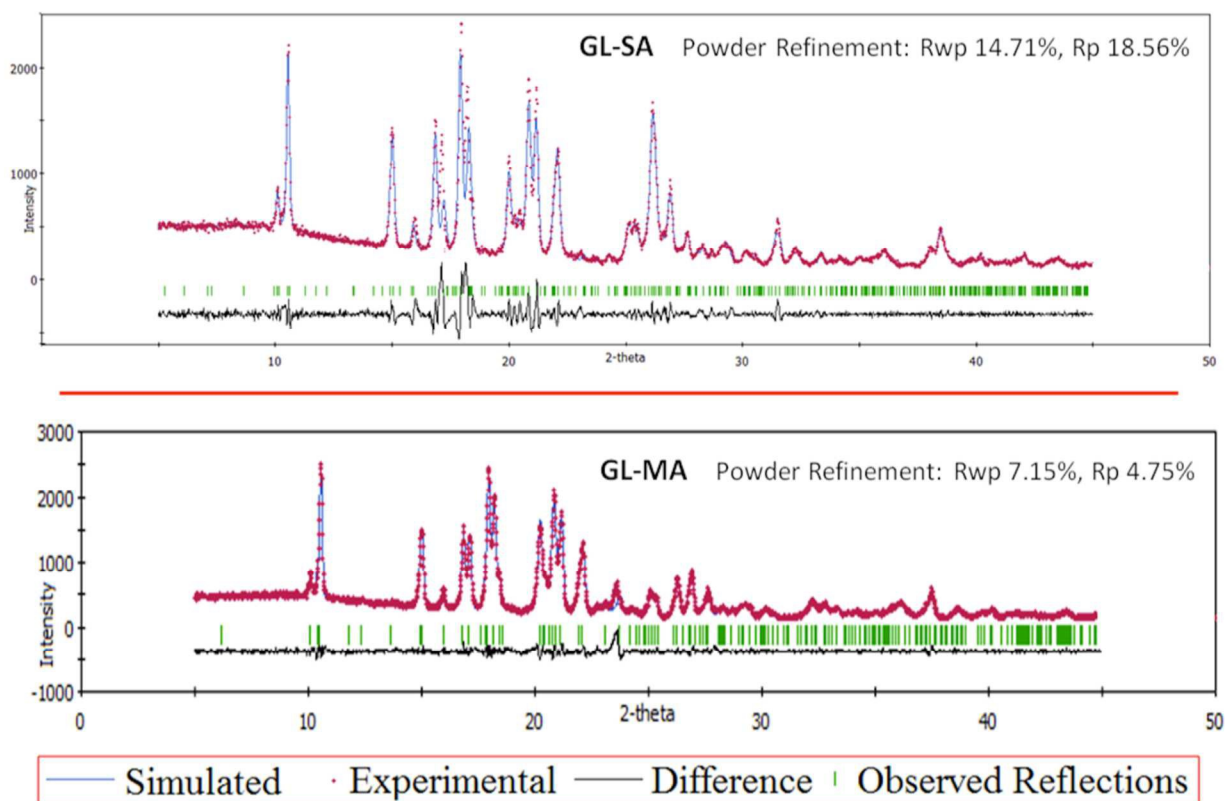
Figure 6 X-ray intensity as a function of 2θ. The simulated (best Rietveld fit profile) pattern, experimental pattern, observed reflections and the difference between simulated and experimental profiles.
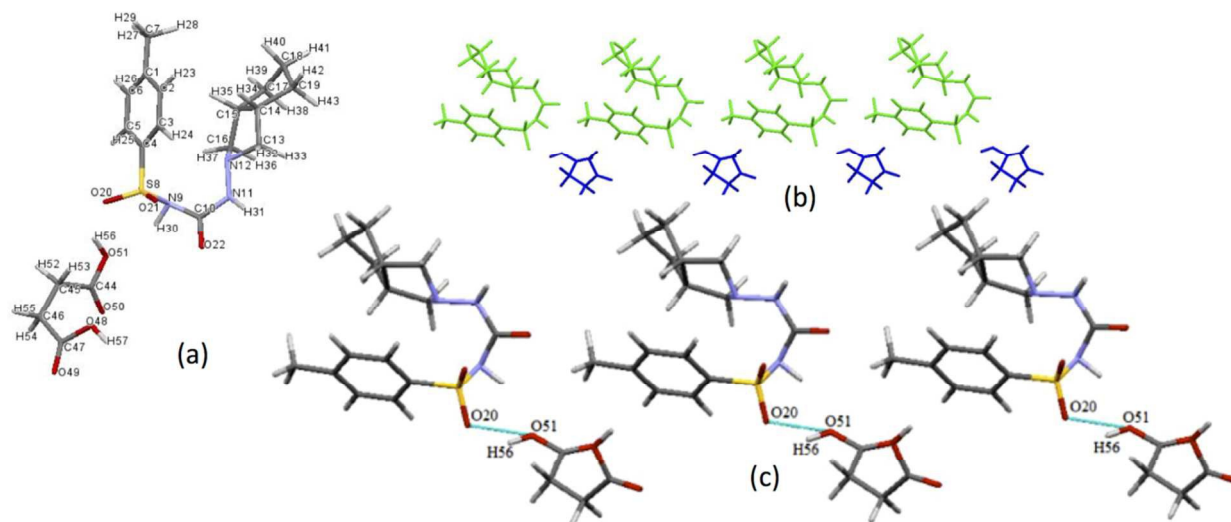
Figure 7 GL-SA (a) asymmetric unit, (b) Crystal packing pattern along b axis, (c) Hydrogen bonded interaction in GL-SA cocrystal

GL-MA crystallizes in the monoclinic system with the space group P2$_1$ /C (R$_{wp}$ = 7.15, Figure 6). The asymmetric unit and packing pattern is given in figure 8. One molecule of GL interacts with three malic acid molecules. —C=O group as well as –OH of carboxylic acid group of MA forms hydrogen bond with –NH (N11–H31···O46) and —C=O of carbamoyl group (O55–H56···O22) of GL, respectively. Another interaction is present between –NH of sulfamoyl and –CO of carboxylic group of another molecule of MA on opposite side (N9–H30···O54). –SO group of GL also shows interaction with –OH of carboxylic group of third molecule of MA (O44–H57···O21).
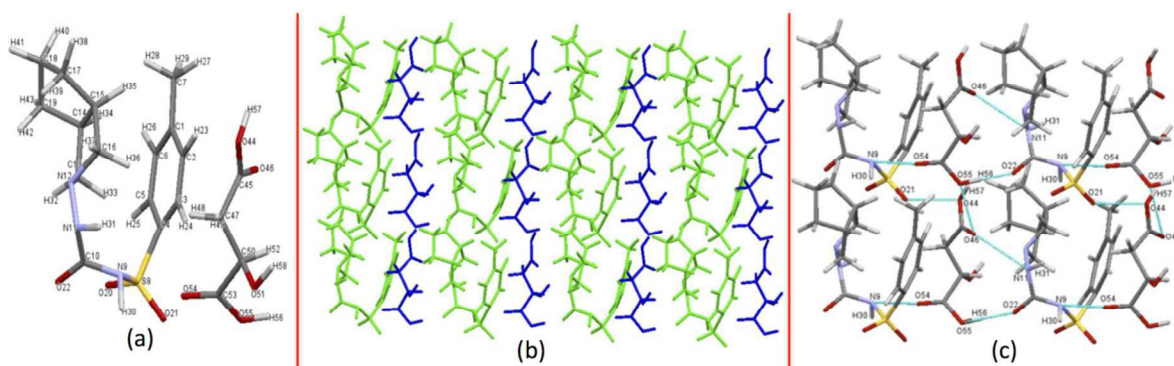
Figure 8 GL-MA (a) asymmetric unit, (b) Crystal packing pattern along b axis, (c) Hydrogen bonded interactions in GL-MA cocrystal

Besides this, two adjacent malic acid molecules are also attached by hydrogen bonds (O55–H56···O46) (Figure 8) serving as both hydrogen bond donor and acceptor. The overall pattern consist of alternate layers of GL and MA molecules.

The crystallographic parameters (Table I) and geometrical parameters (Table II) of GL-MA and GL-SA is given in the table.

The ΔD_{C-O} of C–O and C=O bond distance of carboxyl group of SA is 1.349 Å and 1.196 Å while that of MA is 1.200 Å and 1.364 Å, respectively, which is greater than 0.08Å, suggesting the presence of SA and MA as a neutral molecule in the crystal lattice.

Table I Crystallographic parameters for GL-SA

Parameters	GL-SA	GL-MA
Chemical formula	$C_{15}H_{21}N_3O_3S$	$C_{15}H_{21}N_3O_3S$
Stoichiometry	1:1	1:1
Temperature (K)	Room temperature	Room temperature
Crystal system	Triclinic	Monoclinic
Space group	P_1	$P2_1/c$
a (Å)	13.6952	10.8484
b (Å)	11.1812	14.3701
c (Å)	10.7534	13.0037
α (deg)	82.3900	90.0000
β (deg)	92.5433	125.8402
γ (deg)	90.1698	90.0000
Z	1	4
Vol. (Å3)	1630.54	1643.34
2θ range	5°-45°	5°-45°
R_{wp}	14.71	7.15

Table II Geometrical parameters of GL-MA and GL-SA

D–H···A	r (D–H) (Å)	r (H···A) (Å)	r (D···A) (Å)	∠ D–H···A (deg)
GL-MA				
N9–H30···O54	0.990	2.344	2.554	90.591
O44–H57···O21	0.966	2.953	2.559	57.036
N11–H31···O46	0.999	3.530	2.991	50.240
O55–H56···O22	0.971	1.736	2.564	141.002
O55–H56···O46	0.971	2.854	2.627	--
GL-SA				
O51–H56···O20	0.971	1.736	2.559	140.291

Mechanism of Mechanochemical Cocrystallization

The mechanism of mechanochemical cocrystallization in GL-SA and GL-MA can be explained on the basis of changes at both macroscopic (bulk phase transformation) and microscopic (molecular recognition) levels. In this solvent assisted grinding, the solvent acts as a catalyst and evaporated during the grinding process, which is evident from the absence of any desolvation peak in DSC. Analyzing the PXRD of the ground product at different intervals of time (supplementary data, Figure S2 and S3), witnessed the broadening of a few reflecting peaks, indicating the probable existence of an amorphous intermediate. Although, the solvent was used in the grinding to speed up the reaction, but the formation rate was very slow. The slow rate of formation of cocrystals may be attributed to bulkiness and pretty strong homomeric interaction in GL.

At microscopic level, the mechanism of cocrystallization has been rationalized on the basis of competition of supramolecular synthons that can be formed by the donor or acceptor groups. Gliclazide posses both hydrogen bond-donor (-NH) and -acceptor (-CO and $-SO_2$) groups, making it a potential molecule for cocrystallization. The crystal lattice of pure GL reveals the existence of dimer formation resulting in sulfonamide-sulfonamide and amide-amide homosynthons. However, the incorporation of the co-formers, competed with dimer formation and resulted in the generation of new heterosynthons (Figure 9).

(a)

(b) (c)
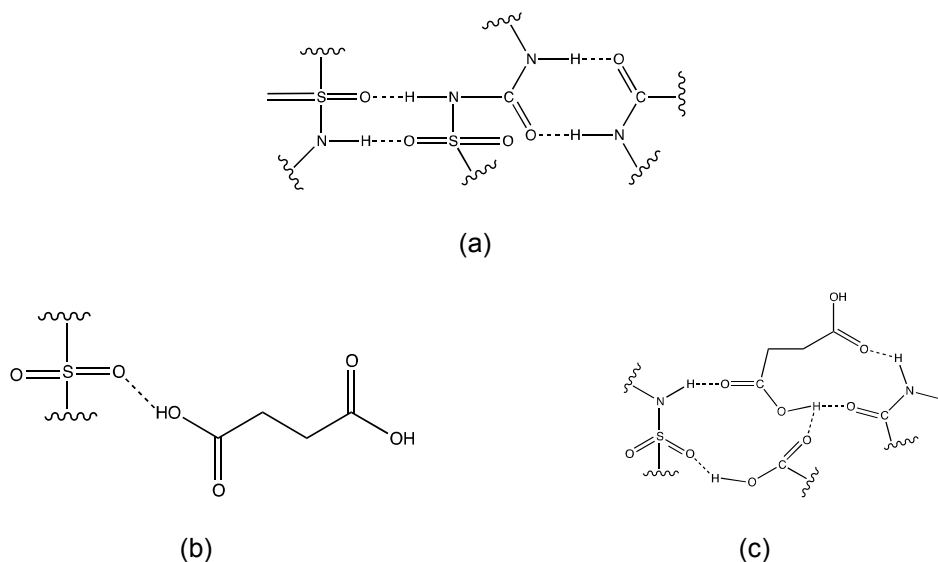
Figure 9 (a) Homosynthons in GL (b) heterosnthon in GL-SA (c) heterosynthon in GL-MA

In case of GL-SA, inclusion of SA in the crystal lattice of GL, disrupted the sulfonamide-sulfonamide and amide-amide homosynthons and formed a single point interaction to GL molecule (O–H⋯O). These

single point attached dyads are stacked over one another through van der Waals forces. In GL-MA, each cocrystallization step involved the opening of sulfonamide-sulfonamide and amide-amide homosynthons and transformation to the three dimensional hydrogen bonded network involving sulfonamide-carboxylic acid and amide-carboxylic acid heterosynthons.

Enthalpy of Solution

The enthalpy of solution provide an insight into the supramolecular architecture of the cocrystals. The contribution of the interaction forces to the cocrystal formation may be deduced by calculating molar enthalpy of solution.

The enthalpy of solution of individual components (drug and coformers) and cocrystals were determined using phosphate buffer pH 7.4 and it was found to be endothermic. The molar enthalpy of solution for cocrystals has been found to be more endothermic than their respective physical mixtures, indicating that more energy is used to break the new lattice (Table III).

Table III Enthalpies of solution, ΔH_{sol}, (kJ mol^{-1})

	ΔH_{sol} (Physical Mixture)	ΔH_{sol} (Cocrystal)
GL-SA	9.26	14.45
GL-MA	8.69	12.60

The formation of cocrystals substantially affects the hydrogen bonded network of the individual componenets, by disrupting the already existing homosynthons and forming new heterosynthons. In case of GL-MA, the lattice is embedded with numerous hydrogen bonds constituting three dimensional networking of molecules, whereas in GL-SA, more endothermic value may be attributed to van der Waals interactions besides hydrogen bonding.

Equilibrium Solubility and Intrinsic Dissolution Studies

The equilibrium concentration and the rate of dissolution are the necessary parameters to be evaluated to assess the developability of the drug and to optimize its performance. Solubility and IDR of GL and its cocrystals (GL-SA and GL-MA) were performed in phosphate buffer pH 7.4, and results are given in table IV. The obtained results demonstrated the comparatively high solubility and IDR of cocrystals, as

compared to GL. Almost 2 fold increase in the solubility and IDR of cocrystals confirmed the improvement

in the physicochemical properties of poorly water soluble drug (GL).

Table IV Solubility and Intrinsic Dissolution Rate (IDR) of GL, GL-SA and GL-MA

	Solubility (mg/mL) ± SD	IDR (mg/min/cm^2) ± SD
GL	2.10 ± 0.2	39.206 ± 0.1
GL-SA	4.49 ± 0.3	48.472 ± 0.2
GL-MA	4.05± 0.2	44.526 ± 0.1

The solubility/IDR is influenced by many factors like melting point, the crystal lattice and the solubility of

the coformers. MA has higher solubility than SA, however, the cocrystal GL-MA exhibited lesser solubility

than GL-SA. The probable reason for this may be the diffrerence in packing of molecules in crystal lattice.

GL-MA has three dimensional hydrogen network, which is difficult to break than two dimensional network

in GL-SA.

In Vivo Studies

The pharmacodynamic study was performed on male Wistar rats and percentage glucose reduction was

measured by GOD – POD (glucose oxidase peroxidase) method. GL-SA and GL-MA showed

considerable glucose level reduction as compared to GL (Table V), as expected from solubility and

dissolution results.

Table V Pharmacodynamic and pharmacokinetic parameters of GL, GL-SA and GL-MA

	Glucose reduction (%) ± SEM	AUC_{0-240} (µg/ml*min)	C_{max} (µg/ml)	T_{max} (min)
GL	75.11 ± 0.2	42542.25	55.26	240
GL-SA	89.46 ± 0.4	84394.65	90.90	240
GL-MA	85.82 ± 0.5	81033.46	81.45	240

Improvement in the solubility and IDR of GL, a BCS class II drug which have dissolution limited

bioavailability, can be correlated with an increase in antidiabetic activity due to high oral bioavailabilty.

This will certainly lead to comparively less dose and consequently less side effects.

The change in physicochemical properties (melting point, solubility etc.) also affects the absorption of the

drug in the body. Tailoring of these paramaetrs would cause the shift in pharmacokinetic paramaters, and

to analyze the same, pharmacokinetic study was performed on male Wistar rats. The concentration of GL

in cocrystals, in plasma at different intervals was calculated and compared with pure GL (Figure 10). All

the pharmacokinetic parameters are given in table V.
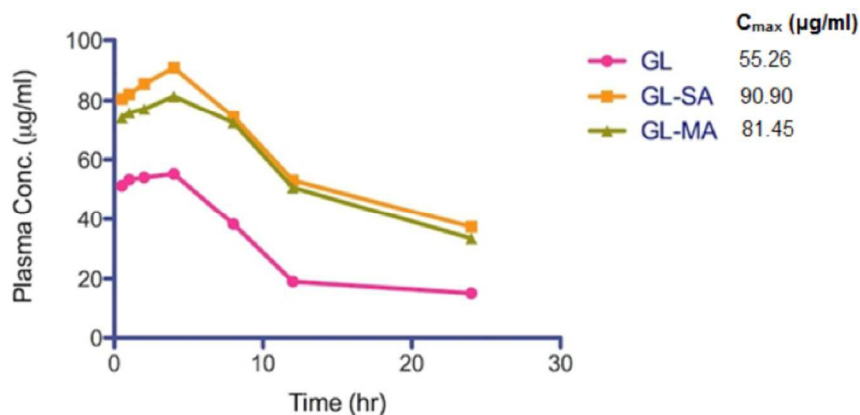
Figure 10 Comparison of plasma concentration of GL, GL-SA and GL-MA

GL-SA and GL-MA showed 1.65 and 1.47 fold increase in C_{max}, respectively as compared to GL.

Although there is a substantial rise in C_{max} but T_{max} remains unaltered, indicating that the extent of

absorption has increased without affecting the rate of absorption.

CONCLUSIONS

The present study illustrates the use of cocrystallization technique for improving the biopharmaceutical

aspects of GL, poorly water soluble drug. Formation of new phase was inferenced from DSC thermogram

and powder diffraction pattern and the same is supported by FTIR . Crystal structure determination from

PXRD pattern using material studio software showed the existence of GL-SA and GL-MA in triclinic (P_1)

and monoclinic ($P2_1/c$) crystal systems respectively. The two new cocrystal (GL-SA and GL-MA) were

found to have relatively high solubility, IDR and remarkable improvement in antidiabetic activity as

compared to GL. The study concludes that the cocrystallization is a viable approach to improve the

biopharmaceutical parameters, hence opening the doors for formulation development of poorly water

soluble drugs.

ACKNOWLEDGEMENT

SUPPORTING INFORMATION

DSC of physical mixtures of GL-SA (1:1) and GL-MA (1:1), PXRD of ground products at different intervals of time.

REFERENCES

1. L. F. Huang and W. Q. T. Tong, *Adv. Drug Delivery Rev.*, 2004, **56**(3), 321-334.

2. B. A. Christer and E. F. Meg, *J. Mol. Pharmaceutics*, 2007, **4**, 317-322.

3. B. Rodríguez-Spong, C. P. Price, A. Jayasankar, A. J. Matzger and N. Rodríguez-Hornedo, *Adv. Drug Delivery Rev.*, 2004, **56**(3), 241-274.

4. S. Y. Lin and S. L. Wang, *Adv. Drug Delivery Rev.*, 2012, **64**(5), 461-478.

5. Ö. Almarsson and M. J. Zaworotko. *Chem. Comm.*, 2004, (17), 1889-1896.

6. S. Mirza, I. Miroshnyk, J. Heinämäki and Yliruusi, *J. DOSIS*, 2008, **24**, 90-96.

7. Y. Chandramouli, R. Gandhimathi, B. R. Yasmeen, A. Vikram, M. B. Dan and S. M. Imroz, *Int. J. Med. Anal*, 2012, **2**(2), 91-100.

8. N. Schultheiss and A. Newman, *Cryst. Growth Des.*, 2009, **9**, 2950–2967.

9. M. L. Peterson, M. B. Hickey, M. J. Zaworotko and Ö. Almarsson, *J. Pharm. Sci.,* 2006, **9**(3), 317-326.

10. K. J. Palmer and R. N. Brogden, *Drugs,* 1993, **46**(1), 92-125.

11. Y. Özkan, T. Atay, N. Díkman, A. Isimer and Y. H. Aboul-Enein, *Pharm. Acta Helv.,* 2000, **74**, 365–370.

12. S. Winters, P. York and P. Timmins, *Eur. J. Pharm. Sci.* 1997, **5**, 209–214.

13. N. P. Sapkal, V. A. Kilor, K. P. Bhusari and A. S. Daud, *Trop. J. Pharm. Res.,* 2007, **6**(4), 833–840.

14. S. Aggarwal, P. N. Singh and B. Mishra, *Pharmazie*, 2002, **57**, 191–193.

15. S. S. Hong, S. H. Lee, Y. J. Lee, S. J. Chung, M. H. Lee and C. K. Shim, *J. Controlled Release,* 1998, **51**, 185–192.

16. S. Biswal, J. Sahoo, P. N. Murthy, P. R. Giradkar and J. G. Avari, *AAPS Pharm. Sci. Tech.*, 2008, **9**(2), 563–570.

17. S. Biswal, J. Sahoo and P. N. Murthy, *AAPS Pharm. Sci. Tech.* 2009, **10**(2), 329–334.

18. S. Biswal, G. S. Pasa, J. Sahoo and P. N. Murthy, *Dissolution Technologies,* 2009, 15-20.

19. P. V. Devarajan and G. S. Sonavane, *Drug Dev. Ind. Pharm.* 2007, **33**(2), 101-111.

20. Averineni, R. Kumar, Shavi, G. Venkatesh, Ranjan, O. Prakash, Deshpande, P. Balavant, Gurram, A. Kumar, Nayak, U. Yogendra, Reddy, S. Meka, Udupa and Nayanabhirama, *Nano Formulation*, 2012, 77-86.

21. J. B. Naik, V. J. Mokale, G. B. Shevalkar, K. V. Patil, J. S. Patil, S. Yadava and U. Verma, *Int. J. Drug Del.*, 2013, **5**, 300-308.

22. C. Winters, L. Shields, P. Timmins and P. York, *J. Pharm. Sci.*, 1994, **83**, 300-304.

23. R. Chadha, A. Saini, P. Arora, S. Chanda and D. V. S. Jain, *Int. J. Pharm. Pharm. Sci.,* 2012, **4**, 244-250.

24. P. Masiello, C. Broca, R. Gross, M. Roye, M. Manteghetti and D. Hillaire-Buys, *Diabetes*, 1998, **47**(2), 224-229.

25. M. Zafar, S. N. H. Naqvi, M. Ahmed and Z. A. Kaimkhani, *Int. J. Morphol.*, 2009, **27**, 783-790.

26. R. Talari, J. Varshosaz, S. A. Mostafavi and A. Nokhodchi, *AAPS Pharm. Sci. Tech.*, 2010, **11**(2), 786-792.

27. Y. Zhang, M. Huo, J. Zhou and S. Xie. *Computer Methods and Programs in Biomedicine*, 2010, **99**, 306–314.

For Table of Content
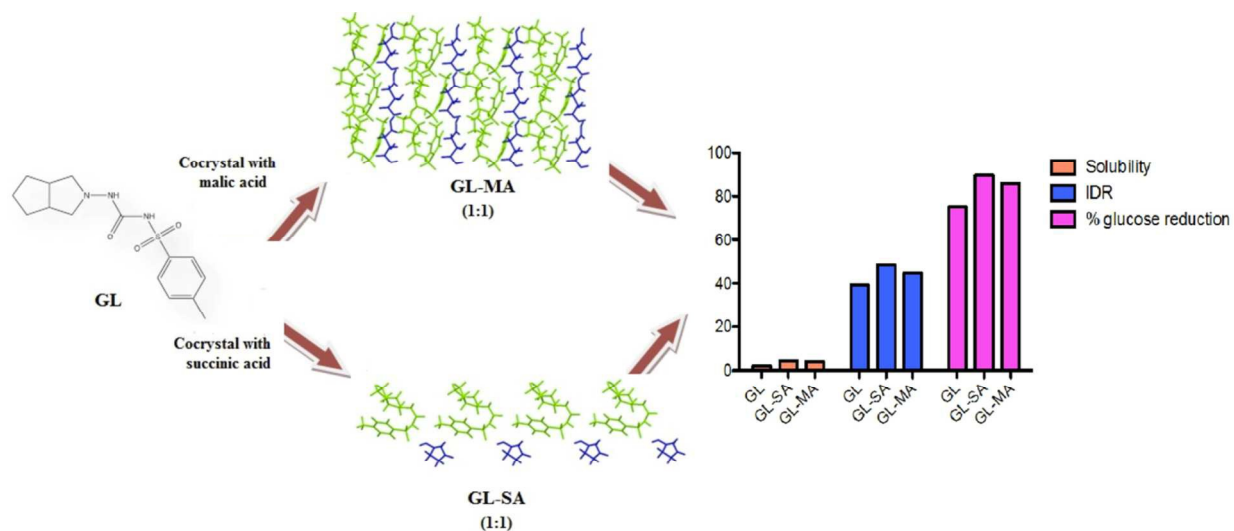
Synopsis

Cocrystallization opens the door for the formulation and development of poorly soluble drugs. Exploiting this technique, the novel cocrystals of gliclazide were formed, displaying noteworthy improvement in solubility, IDR and efficacy in comparison to GL.